FURTHER STUDIES ON IDENTIFICATION OF INELASTIC PARAMETERS FOR DAMAGED MATERIALS

M. VAZ JR. AND M. TOMIYAMA

Department of Mechanical Engineering
State University of Santa Catarina (UDESC)
Campus Universitário Prof. Avelino Marcante, 89219-710 Joinville, Brazil
e-mail: miguel.vaz@udesc.br

Key words: Parameter Identification, Lemaitre damage

Abstract. A proper set of material parameters is one of the most important aspects for a successful simulation of metal forming processes. Several issues must be observed when choosing the constitutive relation and corresponding material parameters, amongst which the most important are: (i) the magnitude of the plastic deformation of the target forming operation must be contemplated by the parameters of the constitutive model, (ii) possibility of failure prediction in fracture-free materials, and (iii) accurate prediction of geometrical changes caused by plastic deformation. Within this framework, the present article discusses techniques to obtain constitutive parameters of a Lemaitre-type material model. The strategy requires compliance of multiple tensile tests with specimens prepared according to different technical standards. Parameter identification is regarded as an inverse problem and solved using optimization methods.

1 INTRODUCTION

Since the pioneering works of Tresca, Huber, von Mises and Hencky [1] on modelling inelastic deformation, many researchers have dedicated much effort to design constitutive formulations able to describe several types of materials, such as polymers, metals and composites amongst many others. Notwithstanding, the determination of the corresponding material parameters have constituted a real challenge. Therefore, for many years, identification of material parameters was based only on mechanical tests assuming uniform stress states. Furthermore, complex constitutive models involving large inelastic deformations, non-uniform stress states and material degradation have posed new demands. In recent years, optimization techniques have been proposed to identification problems aiming at circumventing such difficulties. The present work is inserted within this framework in which an optimization method is used to parameter identification of a Lemaitre-type material model based on tensile tests of specimens of different geometry.

2 MATERIAL MODELLING

The literature shows a growing number of material models able to account for mechanical degradation. In general, such models, known as damaged materials, include new internal variables and evolution laws which are fully coupled to the underlying plasticity problem. The great advantage of damaged materials is the possibility to predict failure onset in actual metal forming operations without pre-defined cracks. Availability of damage models in commercial codes has instigated further investigations on robust and efficient parameter identification strategies. The present work addresses a Lemaitre-type material model, as briefly described in the next session.

2.1 Lemaitre-type damage model

A significant number of damage formulations is based upon thermodynamics of irreversible processes and void growth concepts. Kachanov's [2] and Rabotnov's [3] early works, and Lemaitre's [4] equivalence principle laid foundations for further developments, giving rise to material descriptions oftentimes referred as Continuum Damage Mechanics (CDM). The present work uses an extension of Lemaitre's damage model that accounts for void closure and void opening effects. The reader is referred to [5, 6, 7] for further discussions on the damage formulation.

The present constitutive model requires identification of hardening, $\boldsymbol{p}^h$, and damage, $\boldsymbol{p}^l$, parameters. Swift's [8] hardening equation, $\sigma_Y = k(\bar{\varepsilon}_p + \varepsilon_0)^n$ is adopted in this work, where $\bar{\varepsilon}_p$ is the equivalent plastic strain and $\boldsymbol{p}^h = \{k \, , \, \varepsilon_0 \, , \, n\}$ is the set of hardening parameters. The damage parameters of the model are $\boldsymbol{p}^l = \left\{S \, , \, h^+ \, , \, h^- \, , \, \varepsilon_p^D\right\}$. Therefore, the set of design variables for the present formulation can be generally expressed as $\boldsymbol{p} = \boldsymbol{p}^h \cup \boldsymbol{p}^l$.

3 OPTIMIZATION-BASED PARAMETER IDENTIFICATION

Parameter identification is a class of inverse problems which determines material properties from a known response. The present problem is formulated using unconstrained optimization and accounts for experimental data obtained from tensile tests performed with specimens of different geometry. Therefore, the first step of the optimization problem is formulated as

$$
\begin{aligned}
\text{Minimise} \quad & g(\boldsymbol{p}) = \sum_{s=1}^{n_s} \lambda_s g_s(\boldsymbol{p}) \quad \boldsymbol{p} \in R^{n_d} \\
\text{Such that} \quad & p_i^{\inf} \le p_i \le p_i^{\sup} \qquad i = 1, \ldots, n_d
\end{aligned}
\quad , \tag{1}
$$

where $g(\boldsymbol{p})$ is the global objective function (global fitness), $\boldsymbol{p} = [p_1 \ \ p_2 \ \cdots \ p_i \ \cdots \ p_{n_d}]^T$ is the design vector containing n_d material parameters p_i, and $p_i^{\sup}$ and $p_i^{\inf}$ are lateral constraints. The global fitness, $g(\boldsymbol{p})$, comprises contributions from n_s individual mechanical tests, so that λ_s is the weight function ($\sum_{s=1}^{n_s} \lambda_s = 1$), and $g_s(\boldsymbol{p})$ is the individual fitness and represents a quadratic relative error measure between the experimental, R_s^{Exp}, and

corresponding computed forming load, $R\left(\boldsymbol{p}\right)_s^{Num}$, of a mechanical test "$s$",

$$g_s\left(\boldsymbol{p}\right) = \sqrt{\frac{1}{N_s}\sum_{j=1}^{N_s}\left(\frac{R_{s,j}^{Exp} - R\left(\boldsymbol{p}\right)_{s,j}^{Num}}{R_{s,j}^{Exp}}\right)^2}, \tag{2}$$

in which N_s is the number of experimental points of a mechanical test "s". Particle Swarm Optimization [9, 10] is adopted to solve the optimization problem established in Eqs. (1) and (2) owing to the nature of damage models. Its suitability to this class of problems was extensively discussed in Reference [11].

It is important to note that solution of the optimization problem described in Eqs. (1) and (2) is associated with a given set of weights, λ_s. Inclusion of λ_s as design variable would lead to a set of parameters which provide a minimum for one of the tests only. Therefore, the best set of weights must be determined by an additional optimization problem.

This work proposes a new strategy by comparing the best individual fitness of each test, $g_s^{\min}$, with their counterpart, g_s, calculated evaluated by solution of Eqs. (1) and (2). Therefore, the new optimization problem is solved with weight functions λ_s as design variables, so that

$$\begin{aligned} \text{Minimise} \qquad & G(\boldsymbol{\lambda}) \qquad \boldsymbol{\lambda} \in R^{n_s} \\ \text{Such that} \qquad & 0 \le \lambda_s \le 1 \qquad s = 1, \ldots, n_s \\ & \sum_{s=1}^{n_s} \lambda_s = 1 \end{aligned}, \tag{3}$$

in which $G(\boldsymbol{\lambda})$ is the mean global error,

$$G(\boldsymbol{\lambda}) = \sqrt{\frac{1}{n_s}\sum_{s=1}^{n_s}\left[\frac{g_s^{\min} - g_s(\boldsymbol{p})}{g_s^{\min}}\right]^2}, \tag{4}$$

which expresses a quadratic relative error between the best approximation, $g_s^{\min}$, for each mechanical test and individual fitness, $g_s(\boldsymbol{p})$, obtained by solving the optimization problem established in Eq. (1). It is important to mention that there is a unique relation between the individual fitness and weight for each mechanical test, $g_s(\boldsymbol{p}) \Leftrightarrow \lambda_s$.

Numerical experiments show that the proposed optimization scheme represented by Eqs. (3) and (4) is convex, making possible to use the Nelder-Mead optimization algorithm [12]. The optimization scheme establishes a polytope of $n_s + 1$ vertices, upon which expansion/contraction/shrinkage operations are applied. As the optimization process advances, the polytope moves towards the minimum and decreases in size. Therefore, the mean relative distance between the centrepoint and all vertices of the polytope is used as convergence measure,

$$\phi_d^{(k)} = \frac{d(\boldsymbol{\lambda}^{(k)})}{d(\boldsymbol{\lambda}^{(0)})}, \quad \text{where} \quad d(\boldsymbol{\lambda}^{(k)}) = \frac{1}{n_s + 1}\sum_{j=1}^{n_s+1}\sqrt{\sum_{s=1}^{n_s}\left(\lambda_{j,s}^{(k)} - \bar{\lambda}_s^{(k)}\right)^2}, \tag{5}$$

in which (k) indicates the iterative step, $\bar{\lambda}_s^{(k)} = 1/(n_s + 1) \sum_{i=1}^{n_s+1} \lambda_{s,i}^{(k)}$ is the coordinate of the centrepoint in the direction $s = 1, \cdots, n_s$, and $n_s + 1$ is the number of vertices of the polytope. In this work, convergence is assumed when the initial polytope reduces more than 1,000 times its initial size, i.e. $TOL_d \leqslant 10^{-3}$.

4   NUMERICAL EXAMPLES AND DISCUSSIONS

The identification procedure was performed using tensile tests of cylindrical specimens prepared according to the American ASTM E 8M [13] and Brazilian ABNT NBR ISO 6892 [14] technical standards. Extensometers with initial gauge length $l_0 = 25$ mm or $l_0 = 50$ mm were used according to the specimen with maximum crosshead speed 3 mm/min. The specimens adopted in this work are referred as follows:

- *ASTM #1:* initial gauge length $l_0 = 25$ mm and diameter $d_0 = 6.0$ mm,
- *ASTM #2:* initial gauge length $l_0 = 50$ mm and diameter $d_0 = 12.54$ mm,
- *NBR #3:* initial gauge length $l_0 = 50$ mm and diameter $d_0 = 10.0$ mm,

in which d_0 is the initial diameter.

The geometrical model considers axisymmetry around the rotation axis $Z - Z'$ and symmetry about the $R - R'$ axis, making possible to model only $^1\!/_4$ of the specimen. It was adopted a structured, eight-noded quadrilateral finite element mesh with 200 elements and 661 nodes with progressive refinement towards the specimen $R - R'$ axis. The meshes used for *ASTM #1* e *NBR #3* specimens were geometrically proportional to *ASTM #2* with identical element topology.

Figure 1(a) shows the evolution of the convergence index, ϕ_d, whereas Figure 1(b) presents the corresponding evolution of the weights, λ_s, of the best vertex of the NM polytope. It was assumed $\lambda_s^{(0)} = 1/3$ as initial values. After some variations in the beginning of the iterative process, the optimization scheme quickly leads the weights to the final values. Little change was observed after fourteen iterations and a convergence criterion $TOL_d \leqslant 10^{-2}$ could have been safely adopted (the maximum difference is 0.48 % for λ_1).

The final material parameters, $\boldsymbol{p}$, weights, $\boldsymbol{\lambda}$, and mean global fitness, $G(\boldsymbol{\lambda})$ are presented in Table 1, whereas Figure 2 illustrates the corresponding load evolution. It is noteworthy that the loading curves represent the best approximation to each individual tensile test with parameters determined simultaneously. The results show that geometry still plays a role in determining of inelastic parameters of phenomenological descriptions of plasticity phenomena. However, from industrial viewpoint, the results constitute a good approximation of complex phenomena as material degradation.

5   FINAL REMARKS

Tensile tests have largely been used to determine inelastic parameters. The classical procedure accounts for plastic deformation up to necking onset in order to ensure uniform stress states. However, such condition is achieved for relatively small plastic strains. On the other hand, metal forming operations oftentimes involve large plastic strains.

(a) Convergence index.　　　　(b) Weights, λ_s.
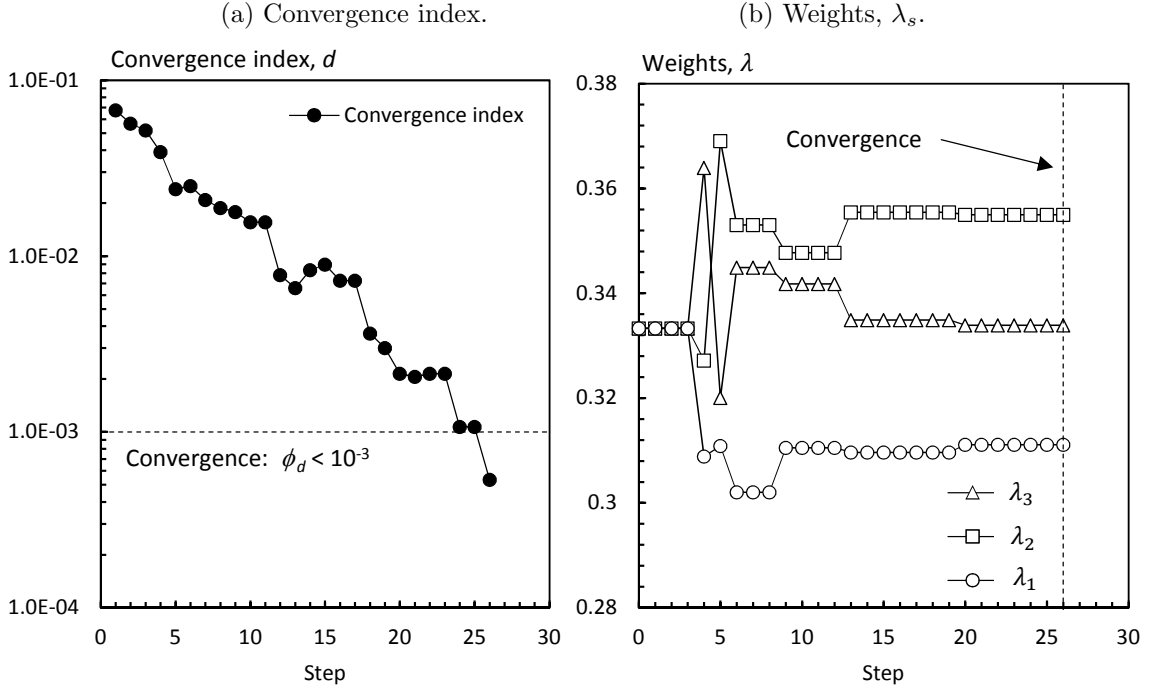
Figure 1: Evolution of the convergence index and weights.

Table 1: Final material parameters, $\boldsymbol{p}$, weights, $\boldsymbol{\lambda}$, and mean global fitness, $G(\boldsymbol{\lambda})$.

	Symbol	Value
Hardening	k	1454.42 MPa
Parameters	ε_0	0.0461830
$\boldsymbol{p}^h$	n	0.414118
Damage	S	889.223 MPa
Parameters	h^-	0.00140679
$\boldsymbol{p}^l$	h^+	1.58511
	ε_p^D	0.402607
Weights	$\lambda_1^{\min}$ (ASTM #1)	0.31112
$\boldsymbol{\lambda}$	$\lambda_2^{\min}$ (ASTM #2)	0.35497
	$\lambda_3^{\min}$ (NBR #3)	0.33390
Global error	$G(\boldsymbol{\lambda}^{\min})$	5.15307

Aiming at such applications, this work uses inverse problem techniques to obtain material parameters up to macroscopic failure. A Lemaitre-type damage model was utilised to assess material degradation e failure.

In general, tensile tests of specimens of a single geometry is adopted. However, aiming at better prediction of the inelastic parameters, this work requires simultaneous compliance of tree tensile tests performed with specimens prepared according to two different technical standards. The inverse problem technique used multi-objective optimization
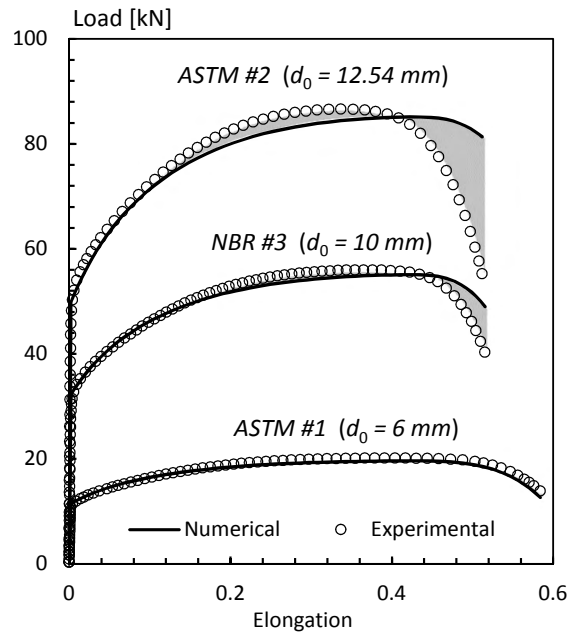
Figure 2: Load evolution for specimens ASTM #1, ASTM #2 and NBR #3.

with the requirement of obtaining the best possible objective function for each individual specimen. Bearing in mind the phenomenological character of the constitutive model, the results indicate a good approximation for all tests. The large discrepancies were found for tensile tests involving the larger tensile loads since the individual objective function has been defined as a relative measure.

Acknowledgements

REFERENCES

[1] Vaz Jr., M., de Souza Neto, E.A. and Muñoz-Rojas P.A. Materials modelling - challenges and perspectives. In: M. Vaz Jr.; E.A. de Souza Neto; P.A. Muoz-Rojas. (Eds.), *Advanced Computational Materials Modeling: From Classical to Multi-Scale Techniques.* Wiley-VCH, 1–22 (2011).

[2] Kachanov, K.M. Time of the rupture process under creep conditions. *Isv. Akad. Nauk. SSR.* (1958) **8**:21–31.

[3] Rabotnov, Y.N. *Creep Problems in Structural Members.* North-Holland, (1969).

[4] Lemaitre, J. A continuous damage mechanics model for ductile fracture. *J. Eng. Mater. Technol., Trans. ASME* (1985) **107**:83–89.

[5] de Souza Neto, E.A., Peric, D., Owen, D.R.J. *Computational Methods for Plasticity. Theory and Applications*. Wiley, (2008).

[6] Vaz Jr., M., de Santi Jr., N., de Souza Neto, E.A. Numerical prediction of ductile failure onset under tensile and compressive stress states. *Int. J. Damage Mech.* (2010) **19**:175–195.

[7] Vaz Jr., M., Munoz-Rojas, P.A., and Lange, M.R. Damage evolution and thermal coupled effects in inelastic solids. *Int. J. Mech. Sci.* (2011) **53**:387–398.

[8] Swift, H.W. Plastic instability under plane stress. *J. Mech. Physics Solids* (1952) **1**:1–18,

[9] Eberhart, R., Kennedy, J. A new optimizer using particle swarm theory. In: *Proceedings of the 6th International Symposium on Micro Machine and Human Science*. IEEE Press, 39–43 (1995).

[10] Kennedy, J., Eberhart, R. Particle Swarm Optimization. In: *Proceedings of the IEEE International Conference on Neural Networks*. IEEE Press, 1942–1948 (1995).

[11] Vaz Jr., M. Particle swarm optimization and identification of inelastic material parameters. *Eng. Comput.* (2013) **30**:936–960.

[12] Nelder, J.A., Mead, R. A simplex method for function minimization, amage evolution and thermal coupled effects in inelastic solids. *The Comput. Journal* (1965) **7**:308–313.

[13] ASTM - E 8M-86a. Tensile testing of metallic materials. ASTM, (2002).

[14] ABNT NBR ISO 6892. Metallic materials - Tensile testing at ambient temperature (in Portuguese). ABNT, (2002).